Articles in PresS. Am J Physiol Endocrinol Metab (September 13, 2016). doi:10.1152/ajpendo.00234.2016

Zinc finger protein 407 overexpression upregulates PPAR-target gene expression and improves glucose homeostasis in mice

Alyssa Charrier[1], Li Wang[1], Erin J. Stephenson[2], Siddharth V. Ghanta[3], Chih-wei Ko[4], Colleen M. Croniger[4], Dave Bridges[2], David A. Buchner[1,3]

Author Contributions. A.C. conception and design of research, performed experiments, analyzed data, interpreted results of experiments, prepared figures, drafted manuscript, edited and revised the manuscript and approved final version of manuscript. L.W. performed experiments, and approved final version of manuscript. E.S. and D.B. performed experiments, edited and revised manuscript and approved final version of manuscript. S.G. performed experiments, analyzed data, interpreted results of experiments, approved final version of manuscript. C.K. performed experiments, revised manuscript, and approved final version of manuscript, C.M.C. performed experiments, revised manuscript, and approved final version of manuscript, D.A.B. conception and design of research, analyzed data, interpreted results of experiments, edited and revised the manuscript and approved final version of manuscript. D.A.B. is the guarantor of this work and, as such, takes responsibility for the integrity of the data and the accuracy of the data analysis.

[1]Department of Genetics and Genome Sciences, Case Western Reserve University, Cleveland, OH 44106, [2]Department of Physiology, University of Tennessee Health Science Center, Memphis, TN 38163, Department of Pediatrics, University of Tennessee Health Science Center, Memphis, TN 38103. [3]Department of Biochemistry, Case Western Reserve University, Cleveland, OH 44106. [4]Department of Nutrition, Case Western Reserve University, Cleveland, OH 44106

Running Head: Zfp407 improves glucose homeostasis

Address for reprint requests and other correspondence:
David Buchner, Case Western Reserve University, 10900 Euclid Ave., Cleveland, OH 44106
Phone: 216-368-1816
Email: dab22@case.edu

Abstract

The peroxisome proliferator-activated receptor (PPAR) family of nuclear receptors are central to the pathophysiology and treatment of metabolic disease through their ability to regulate the expression of genes involved in glucose homeostasis, adipogenesis, and lipid metabolism. However, the mechanism by which PPAR is regulated remains incompletely understood. We generated a transgenic mouse strain (ZFP-TG) that overexpressed Zfp407 primarily in muscle and heart. Transcriptome analysis by RNA-Seq identified 1,300 differentially expressed genes in the muscle of ZFP-TG mice, among which PPAR target genes were significantly enriched. Among the physiologically important PPARγ target genes, Glucose transporter (Glut)-4 mRNA and protein levels were increased in heart and muscle. The increase in Glut4 and other transcriptional effects of Zfp407 overexpression together decreased body weight and lowered plasma glucose, insulin, and HOMA-IR scores relative to control littermates. When placed on high fat diet, ZFP-TG mice remained more glucose tolerant than their wild-type counterparts. Cell-based assays demonstrated that Zfp407 synergistically increased the transcriptional activity of all PPAR subtypes, PPARα, PPARγ, and PPARδ. The increased PPAR activity was not associated with increased PPAR mRNA or protein levels, suggesting that Zfp407 post-translationally regulates PPAR activity. Collectively, these results demonstrate that Zfp407 overexpression improved glucose homeostasis. Thus, Zfp407 represents a new drug target for treating metabolic disease.

Introduction

Type 2 diabetes affects nearly 300 million individuals worldwide (30). Complications of type 2 diabetes include cardiovascular disease, neuropathy, nephropathy, and retinopathy, among others. Central to the pathophysiology of type 2 diabetes is the insulin resistance of peripheral tissues including adipose, liver, and muscle that is defined by decreased insulin-stimulated glucose uptake. These changes are also associated with altered levels of cytokine and fatty acid release and elevated inflammation (7, 29).

Zinc finger protein 407 (Zfp407) was identified as a regulator of insulin-stimulated glucose uptake during a siRNA screen performed in 3T3-L1 adipocytes (10). Zfp407 is predicted to encode a 246 kDa protein with 24 zinc finger domains. Zfp407 knockdown in adipocytes reduced insulin-stimulated glucose uptake and decreased expression of peroxisome proliferator-activated receptor (PPAR)-γ-target genes including the glucose transporter GLUT4 (10). The PPAR family of nuclear hormone receptors, which includes PPARα, PPARγ, and PPARδ, are central to the pathophysiology and pharmacological treatment of insulin resistance (20). Genetic variation in all 3 PPAR family members is associated with altered insulin sensitivity in humans demonstrating their importance in regulating glucose homeostasis (2, 6, 11, 38).

PPARγ expression is highest in adipocytes, where it controls adipogenesis and lipid homeostasis (1). PPARγ functions in other tissues by enhancing anti-immune responses and lipid metabolism in macrophages, increasing lipid storage in liver, and enhancing glucose-stimulated insulin secretion in pancreatic β-cells (1). PPARα is expressed highest in the liver and promotes fatty acid oxidation (35). PPARα regulates energy store

management in the liver during fasting (21). PPARδ, which is widely expressed, regulates fatty acid catabolism and energy homeostasis in adipose tissue and muscle and suppresses macrophage-derived inflammation (5).

While PPAR family members each have unique expression patterns, all 3 are expressed together in skeletal muscle tissue (9). Muscle is the major contributor of postprandial glucose uptake and accounts for nearly 91% of all glucose uptake (12). PPAR activity in muscle is necessary for maintaining glucose homeostasis as muscle-specific PPARγ deficiency in mice leads to insulin resistance (18, 27). Additionally, PPARγ or PPARδ overexpression in muscle improves whole body insulin sensitivity (3, 39). Further, PPARα muscle-specific overexpressing mice were glucose intolerant, but still protected from diet-induced obesity (15). It is clear that in skeletal muscle each PPAR family member has non-redundant contributions to maintaining whole body glucose homeostasis (3, 15, 18, 27, 39).

Zfp407 positively regulates the transcription of PPARγ target genes in the 3T3-L1 adipocyte cell line (10). However, the *in vivo* and tissue specific effects of Zfp407 on organismal physiology and pan-PPAR signaling have not been tested. Thus we generated a new transgenic mouse strain that primarily overexpresses Zfp407 in muscle to test whether Zfp407 can modulate the PPAR family of nuclear receptors *in vivo* and improve whole body glucose homeostasis.

Materials and Methods

Cell Culture. Dulbecco's Modified Eagle's Medium (DMEM), Fetal bovine serum, L-Glutamine/Pen/Strep, 0.05% Trypsin-EDTA, were obtained from Life Technologies (Carlsbad, CA, USA). 293T cells cultured in DMEM with 10% FBS and 1x L-Glutamine/Pen/Strep.

Mice. Zfp407 transgenic mice were generated on a C57BL/6J background at the Case Transgenic and Targeting Core with a linearized mouse DNA fragment encoding a Myc/DDK-tagged Zfp407 protein under the control of a CMV promoter. Mice were housed in ventilated racks with access to food and water *ad libitum* and maintained at 21°C on a 12-hour light/12-hour dark cycle. All mice were cared for as described under the Guide for the Care and Use of Animals, eighth edition (2011) and all experiments were approved by IACUC and carried out in an AAALAC approved facility. Mice were fed standard chow diet LabDiet 5010 unless otherwise indicated (PMI Nutrition International, St. Louis, MO, USA). For dietary studies mice were fed either a high fat/high sucrose diet (HFD) with 58% of kcal from fat or a nutritionally balanced control diet (CD) with 10.5% of kcal from fat (D12331 (HFD) and D12328 (CD), Research Diets, New Brunswick, NJ, USA). Wild type (nontransgenic) C57BL/6J littermates were used as controls for all mouse experiments. For metabolic studies, mice were fasted 16 hours overnight and blood glucose levels were measured via retro orbital bleeds. Whole blood was collected by cardiac puncture using BDmicrotainer tubes with K_2 EDTA. Body composition was determined non-invasively using an echo-MRI 1100 (33). For tissue collection, mice were anesthetized with isofluorane and euthanized by cervical

dislocation at 9 am (ZT3). Tissues were either snap frozen in liquid nitrogen or placed in RNAlater (Thermo Fisher Scientific, Waltham, MA, USA).

Glucose and Insulin Tolerance Test. Following 86 days on the HFD or CD, mice were fasted overnight for 16 hours, blood samples were collected by tail vein nick, and glucose levels were measured with a handheld glucometer at baseline (time 0) and following intraperitoneal injection of dextrose (2 g/kg body weight) or insulin (1U/kg body weight) dissolved in water or PBS, respectively.

RNA Analysis. RNA was isolated using the PureLink RNA purification kit with TRIzol protocol (Thermo Fisher Scientific, Waltham, MA, USA). Total RNA was reverse transcribed using the high capacity cDNA reverse transcription kit without the RNase inhibitor (Applied Biosystems, Carlsbad, CA, USA). Primer sequences for detecting endogenous (primers in the 3'UTR), transgene (reverse primer in the myc tag) or total Zfp407 (primers in exon 2 and 3) mRNA were as follows: endogenous Zfp407 forward primer: 5'-CCACG GAACT TTGTC GTGTT-3', endogenous Zfp407 reverse primer: 5'-TGCTC TATGG CACAG GTTCA-3', transgene Zfp407 forward primer: 5'-CACAG TGATC CAGAG CCAAA-3', transgene Zfp407 reverse primer: 5'-TTGCT GCCAG ATCCT CTTCT-3', total Zfp407 forward primer: 5'-GAGAG GAGAA CCAGG GCAAC-3', and total Zfp407 reverse primer: 5'-CCTCA TCCCA AGGTG CCTTT-3'. All other primer sequences were previously published (10). qPCR reactions were performed with the power SYBR green PCR Master Mix and run on a Bio Rad CFX Connect Real Time System (Bio Rad, Hercules, CA, USA). Expression levels were

calculated using the ΔΔCt method relative to the *Arbp* control gene. For RNA-Seq analysis, total RNA was isolated as described above with an additional on-column DNase treatment step. RNA quality was determined on the Agilent BioAnalyzer 2100 and all samples had an RNA integrity number score greater than 9.5. Illumina TruSeq sequencing libraries were prepared at the CWRU genomics core. Samples were run on an Illumina HiSeq2500 with an average of 41,923,675 reads per sample (range: 32,620,433-51,759,718). Reads were aligned to the mouse genome (Ensembl m38.82) using TopHat v2.1, SamTools v1.2, and Bowtie v2.2.6 (22, 24, 25). Gene expression count tables were generated using HTSeq v0.6.1 (4) and analyzed for differential expression by DESeq2 v1.10 (26). Heatmaps were generated in R version 3.2.2 with the heatmap.2 function in the gplots package v2.17. GO analysis was conducted at geneontology.org (17). Enriched KEGG pathways were identified using Molecular Signatures Database (34). A FDR adjusted $p < 0.05$ was considered statistically significant for RNA-Seq analyses. The RNA-Seq expression profiling data is available in the Gene Expression Omnibus series GSE83541.

Western blotting. Western blotting was performed and quantitated as described (10). Anti-GLUT4 (2213) and anti-PPARγ (2430 and 2443) antibodies were from Cell Signaling (Danvers, MA, USA). Anti-PPARδ (60193-1) and anti-PPARα (15540-1) were from Proteintech Group (Rosemont, IL, USA). Anti-GAPDH (MA5-15738) was from Thermo Fischer Scientific (Waltham, MA, USA). A custom anti-ZFP407 antibody was generated in rabbit against the C-terminal 149 amino acids of the mouse ZFP407 protein

(Proteintech Group, Rosemont, IL, USA). Goat anti-rabbit (31460) and goat anti-mouse (31430) secondary antibodies were from Thermo Fisher Scientific (Waltham, MA, USA).

Plasma metabolites. Plasma insulin concentrations were determined using the Ultra Sensitive Mouse Insulin ELISA Kit (Crystal Chem, Inc, Downers Grove, IL, USA). Beta-hyroxybutyrate, cholesterol, triglyceride, and nonesterified fatty acids were measured at Marshfield Labs (Marshfield, WI, USA). HOMA-IR scores were calculated using the following equation: insulin (μU/ml) x glucose (mg/dl) / 405.

Muscle triglyceride analysis. Mouse skeletal muscle (biceps femoris) (70-100 mg) was saponified with an equal volume by weight of 3M KOH/65% ethanol. The sample was incubated at 70°C for 1 h and then room temperature for 24 h. The sample volume was adjusted to 300 μl of 50 mM Tris per 100 mg of tissue used. Glycerol concentration was measured against glycerol standards using a commercially available triglyceride glycerol phosphate oxidase (GPO) reagent kit (Pointe Scientific, Lincoln Park, MI, USA).

PPAR luciferase reporter assay. 293T cells were transfected using Lipofectamine 3000 (Life Technologies, Carlsbad, CA, USA). DNA plasmid constructs transfected encoded PPARγ (Addgene #8862 (37)), PPARδ (36), PPARα (36), ZFP407 (MR214555, Origene Technologies, Rockville, MD, USA), an empty vector control plasmid (pRK5-Myc), and the PPAR target gene luciferase reporter plasmid (Addgene #1015 (23)). 490 ng of DNA from the above plasmids was transfected per well with 10 ng of pRL-SV40 encoding

Renilla for normalization. Luciferase and Renilla were measured 24 hours post transfection with the Dual-Glo Luciferase Assay System (Promega, Madison, WI, USA).

Histology. Mouse skeletal muscle (biceps femoris) and heart tissues were fixed in 10% v/v neutral buffered formalin, embedded in paraffin, sectioned, and stained with haematoxylin & eosin by the Case Tissue Resources Core. Succinate dehydrogenase staining (SDH) and alpha glycerol-3-phosphate dehydrogenase (GPDHα) stains performed on cryosections as described (13). Semi-quantification of fiber intensity was performed on a blinded basis using a scale of 0-4 (0, no staining and 4, most intense staining) by two individual scorers (n=3 samples per group with 5 random pictures taken per sample at 200x magnification). Final counts were normalized and analyzed by Student's t-test.

Genotyping and transgene copy number determination. Transgenic Zfp407 mice were genotyped using a 3-primer PCR reaction that amplifies a single 156 base pair DNA fragment in wild-type (WT) mice and an additional 396 base pair fragment in transgenic mice. Forward primer: 5'-TCTGT GACCT CTGTG GCTTC-3', Reverse primer 1: 5'-AAGCA AACCA TAGGA CTTGG ACA-3', Reverse primer 2: 5'-GGCAC TCATA GGACT TGGAC A-3'. Copy number of the Zfp407 transgene was determined as previously described (19) using the following primer pair: exon 1 forward primer: 5'-CCAAC CCACA GGCAC CCTGC-3' and exon 1 reverse primer: 5'-ACTCG GACGG TGTTG CTGCG-3'.

Statistics. Data are shown as the mean ± standard error unless otherwise indicated. Western blot, qPCR, and muscle triglyceride data were analyzed by two-tailed Student's t-test. Glucose tolerance tests were analyzed by repeated measures ANOVA followed by Bonferroni's correction for multiple comparison. The physiological parameters described in Table 1 were analyzed by a two-way ANOVA for effects of genotype and sex. The physiological parameters described in Tables 2 and 3 were analyzed by a three-way ANOVA for effects of genotype, sex and diet. For all physiological parameters listed in Tables 1-3, a sample size of $n \geq 75$ was considered large enough to assume normal distribution by histogram visualization. When the sample sizes were $n < 75$, a Shapiro-Wilk test for normal distribution was performed on the residuals of the ANOVA analysis. If a trait failed normality ($p < 0.05$) than values were reshaped by taking the natural log. The reshaped values all passed the Shapiro-Wilk test for normal distribution and so ANOVA was performed on these values. P values < 0.05 were considered statistically significant for all statistical tests.

Results

ZFP-TG mice overexpress Zfp407 in heart and muscle. A new strain of transgenic mice (ZFP-TG) was generated that carry a transgene encoding a Myc/DDK-tagged Zfp407 protein under the control of a CMV promoter (Fig. 1A). The transgene was injected into fertilized one-cell embryos from the strain C57BL/6J, upon which it randomly inserted into the genome. ZFP-TG mice have 11.5 ± 1.32 exogenous copies of the Zfp407 cDNA in addition to the 2 endogenous copies of the gene. ZFP-TG mice were viable with no obvious morphological defects, although a slight deficiency of

243 female ZFP-TG hemizygous mice was observed relative to the expected number of
244 transgenic offspring in a backcross (Chi-square: females, $p < 0.05$; males, $p > 0.1$).
245 Endogenous Zfp407 mRNA levels were unchanged between ZFP-TG and WT mice in all
246 tissues, whereas most tissues examined in ZFP-TG did express the transgene at varying
247 levels, with the highest expression occurring in heart and muscle (Fig. 1B, C). Total
248 Zfp407 mRNA expression was significantly increased in gonadal and subcutaneous
249 adipose tissue, brain and kidney (Fig. 1D). Additionally, the highest expression levels
250 occurred in the heart and muscle with a 3.0- and 19.3-fold increase, respectively (Figure
251 1D). A corresponding 4.0- and 67-fold increase in Zfp407 protein levels were detected in
252 heart and muscle, whereas no other tissue had significantly increased levels of Zfp407
253 protein (Figure 2). Therefore, Zfp407 is primarily overexpressed in heart and skeletal
254 muscle, although there may be additional small increases in Zfp407 protein levels in
255 tissues such as brain and kidney and we cannot exclude the possibility of Zfp407
256 overexpression in other cell and tissue types not tested.

257 To determine whether increased ZFP407 protein levels affected heart or muscle gross
258 morphology, sections of these tissues from male and female mice were stained by
259 haematoxylin & eosin and blindly analyzed by a pathologist. No structural differences
260 were detected and there were no overt changes in inflammatory cell infiltration between
261 WT and ZFP-TG tissue (Fig. 3A, B). Gene expression based markers of slow-twitch
262 (*Atp2a1*) and fast-twitch (*Atp2a2*) fibers did not differ between ZFP-TG and control
263 strains (Fig. 3C). Further, SDH (more oxidative, slow twitch fibers) and GPDHα (more
264 glycolytic, fast twitch fibers) staining intensities did not differ between WT and ZFP-TG

muscle tissue (Fig. 3D, E), suggesting that there was no difference in the distribution of fast- and slow-twitch muscle fibers.

Transcriptome changes in ZFP-TG muscle. Whole transcriptome analysis of muscle tissue was undertaken to identify downstream target genes regulated by Zfp407. Hierarchical clustering of the muscle transcriptome of ZFP-TG and control mice showed distinct patterns of gene expression, demonstrating widespread transcriptional changes induced by Zfp407 overexpression (Fig. 4A). There were 1,300 genes differentially expressed between ZFP-TG and control mice including 901 upregulated and 299 downregulated (Fig. 4B, Supplemental table 1). Zfp407 was the most statistically significantly upregulated gene, with a 21-fold increase in ZFP-TG muscle (Supplemental table 1).

Gene Ontology analysis of differentially expressed genes identified a number of significantly upregulated pathways including cholesterol, steroid and fatty acid metabolic processes, antigen processing and presentation and complement activation (Fig. 4C). Analysis of KEGG pathways among the differentially expressed genes demonstrated that genes within the PPAR signaling pathways were significantly enriched ($p = 4.0 \times 10^{-6}$) (Supplemental table 2). As PPAR pathway genes were significantly enriched among the differentially expressed genes, and Zfp407 was previously implicated in PPAR signaling (10), we examined the expression of all genes within the PPAR KEGG pathway. PPAR pathway genes were consistently upregulated in the ZFP-TG mice relative to controls (Fig. 4D). Among the key PPAR target genes in the muscle, Plin2 and Angptl4 expression was significantly upregulated by Zfp407 overexpression, while Pdk4 demonstrated a trend toward increased expression in the muscle of ZFP-TG mice (Fig.

288 5C) (8, 32, 40). However, levels of PPARα, PPARγ, and PPARδ mRNA and protein did
289 not differ between ZFP-TG and WT mice (Figs. 4B, 5A).

290 Other KEGG pathways that were enriched included retinol, drug and linoleic acid
291 metabolism and the complement and coagulation cascades (Supplemental table 2). The
292 differentially expressed genes in these KEGG pathways were typically expressed
293 specifically in the liver, but were consistently activated in the muscle by Zfp407
294 overexpression. Among these liver-specific genes were hepatic nuclear factor 4 alpha
295 (HNF4α) and 61 HNF4α-target genes (Supplemental table 3). This suggests that Zfp407
296 may drive expression of this pathway which is critical for gene expression programming
297 of hepatocytes (28, 31).

298 **Zfp407 positively regulates pan-PPAR activity.** While Zfp407 positively regulates the
299 activity of PPARγ (10), it was not known whether this also true for PPARα or
300 PPARδ and whether this regulation would be mediated via the canonical PPRE element.
301 To test whether Zfp407 controls the activity of PPARα and PPARδ, Zfp407 was co-
302 expressed with these PPARs and the PPRE-containing PPAR luciferase reporter plasmid.
303 Co-overexpression of PPARα or PPARδ with Zfp407 resulted in a 1.5 ± 0.1 and 2.1 ±
304 0.2–fold increase, respectively, in luciferase activity relative to each PPAR alone (Fig.
305 5B). Thus, Zfp407 positively regulates PPRE-dependent expression with all three
306 PPARs.

307 **Zfp407 overexpression increased Glut4 levels.** A significant increase in Glut4 mRNA
308 in ZFP-TG muscle was detected by both RNA-Seq and qPCR (Fig. 6A-B). Glut4 protein
309 levels were also increased in the heart and muscle of ZFP-TG mice, where Zfp407

310 protein levels were increased, but not in subcutaneous adipose tissue where Zfp407
311 protein levels were unchanged (Fig. 6C). Thus, the increase in Glut4 expression due to
312 Zfp407 overexpression is likely cell autonomous.

313 **Improved glucose homeostasis in ZFP-TG mice.** Two-way ANOVA analysis of
314 metabolic data collected at 5 weeks of age for both male and female chow-fed ZFP-TG
315 and littermate nontransgenic control mice demonstrated that Zfp407 overexpression
316 effects body weight, body length (nose to tail), fasting glucose, fasting insulin and
317 HOMA-IR (Table 1). Male and female ZFP-TG mice weighed less and were smaller
318 (body length) than their WT littermates (Table 1). Both male and female ZFP-TG mice
319 had decreased fasting plasma glucose levels, lower fasting plasma insulin levels, and
320 lower HOMA-IR scores (Table 1). Collectively, this metabolic data demonstrates that
321 ZFP407 overexpression improves fasting markers of glucose homeostasis. Cholesterol,
322 triglycerides and nonesterified fatty acids (free fatty acids) were unchanged in the plasma
323 of ZFP-TG mice. However, two-way ANOVA demonstrated an effect of Zfp407
324 overexpression on plasma beta-hydroxybutyrate (representative of ketone bodies) levels,
325 which were increased in both male and female ZFP-TG mice relative to controls (Table
326 1). The increase in plasma beta-hydroxybutyrate levels can potentially be due to
327 increased adipose lipolysis associated with increased fatty acid uptake by the liver or are
328 due to physiological changes in the muscle.

329 **Improved glucose tolerance in HFD-fed ZFP-TG mice.** Three-way ANOVA analysis
330 of metabolic data collected following 100 days of CD or HFD feeding in male and female
331 ZFP-TG and control mice demonstrated that Zfp407 overexpression effects final body
332 weight and total weight gained, but not the percent weight gained. Whereas ZFP-TG

mice weighed less than their WT littermates, their percent body weight gained during CD- or HFD-feeding did not differ (Table 2). Additionally, plasma cholesterol levels were decreased in both male and female HFD-fed ZFP-TG mice. Muscle triglyceride levels did not differ between WT or ZFP-TG HFD-fed female mice (Table 2).

Fasting blood glucose levels were also lower in male and female ZFP-TG mice, however there was no effect of Zfp407 overexpression on insulin levels or HOMA-IR scores (Table 2). Nonetheless, CD-fed male ZFP-TG mice were more glucose tolerant than WT littermates as were both male and female ZFP-TG mice fed the HFD for 100 days (Fig. 7). Remarkably, the HFD-fed ZFP-TG mice remained as glucose tolerant as the CD-fed littermates, whereas WT mice fed the HFD became insulin resistant (Fig. 7). These data indicate that Zfp407 overexpression improves glucose homeostasis under obesogenic conditions.

Discussion

We describe a new transgenic mouse strain that overexpresses Zfp407 resulting in improved whole body glucose homeostasis. The improved metabolic profile is associated with the first demonstration that Zfp407 broadly regulates the expression of PPAR target genes *in vivo*, although the physiological phenotype associated with Zfp407 overexpression differs from other models of increased PPAR activity in the muscle. Muscle-specific PPARγ overexpression increased insulin sensitivity due to endogenous activation of adiponectin. This was associated with a higher percentage of oxidative muscle fibers but no change in body weight (3). PPARδ muscle-specific overexpression

355 also increased the proportion of slow twitch type I (oxidative) muscle fibers as compared
356 to fast twitch (glycolytic) fibers, resulting in enhanced exercise endurance (39). The
357 PPARδ transgenic mice were also protected from diet-induced obesity and were insulin
358 sensitive relative to control mice (39). PPARα muscle-specific overexpression increased
359 fatty acid oxidation rates and protected from diet-induced obesity, but these mice
360 remained glucose intolerant (15). Taken together, the differences and similarities
361 observed between each of the PPAR overexpressing mice and our Zfp407 overexpressing
362 mouse suggests that while Zfp407 does regulate the activity of the PPAR proteins, the
363 combinatorial effect of pan-PPAR activation by Zfp407 or potentially other molecular
364 pathways likely underlie the improvements in glucose homeostasis, rather than the
365 specific activation of a single PPAR family member.
366
367 Zfp407 overexpression was also sufficient to induce HNF4α expression in the muscle,
368 where it is not typically expressed, and with it the widespread activation of many liver-
369 specific genes. This presumably non-physiologic induction of HNF4α and its target
370 genes demonstrates that Zfp407 overexpression alone is sufficient to induce a broad liver-
371 specific transcriptional program within the context of a muscle cell, thus providing
372 insight into its potential downstream target genes. Like other nuclear superfamily proteins
373 such as PPARγ and RXRα, HNF4α binds to the classical DR1 binding motif (14). It is
374 interesting to note that expression of the PPARs is not upregulated by Zfp407, whereas
375 HNF4α was upregulated at the mRNA level. Yet both HNF4α and PPARs activate gene
376 expression by hetero-dimerizing with RXRα and binding to the DR1 consensus sites.
377 Thus, while we hypothesize that Zfp407 enhanced PPAR target expression through

posttranslational effects on the PPARs, it is not clear as to whether Zfp407 has similar posttranslational effects on other nuclear receptors such as HNF4α.

The overexpression of Zfp407 in ZFP-TG mice appeared to be restricted to the cardiac and skeletal muscle (Fig. 2). The CMV promoter used to drive Zfp407 overexpression typically drives expression in all tissues, although levels can vary greatly between tissue type (16). Therefore, it remains possible that the phenotypic outcomes observed may be due to Zfp407 overexpression in tissues or cells beyond just muscle and heart. Based on the metabolic improvements of ZFP-TG mice, it will be of interest to test additional Zfp407 transgenic mouse models utilizing more highly tissue-specific promoters. It is also important to note that the effects of Zfp407 overexpression could be supraphysiological in nature, nonetheless, the fact that Zfp407 overexpression in muscle tissue results in a reciprocal effect on PPAR target gene expression relative to the effects of Zfp407 inhibition in cultured adipocytes (10) suggests that Zfp407 controls pan-PPAR signaling in multiple tissues. Taken together these results suggest that Zfp407 regulates the transcription of multiple pathways including the PPAR and HNF4α pathways, among others.

Grants. This work was supported by NIH grants DK099533 and DK084079 to D.A.B.. and DK107535 to D.B.. D.B. was also supported by funds from the Memphis Research Consortium. A.C received a postdoctoral fellowship grant (#1-16-PDF-018) from the American Diabetes Association.

Acknowledgements. The authors thank Dr. Ron Conlon and the Case Western Reserve University Transgenic and Targeting Facility for generating the ZFP-TG strain, Drs. Noa Noy (Cleveland Clinic Lerner Research Institute) and Hung-Ying Kao (Case Western Reserve University) for providing plasmids, and Dr. Yuying Jiang (Case Western Reserve University) for assistance in tissue pathology analysis.

Present address of D. Bridges: Department of Nutritional Sciences, University of Michigan School of Public Health, Ann Arbor, MI 48109 (e-mail: davebrid@umich.edu).

References

1. **Ahmadian M, Suh JM, Hah N, Liddle C, Atkins AR, Downes M, and Evans RM**. PPARgamma signaling and metabolism: the good, the bad and the future. *Nature medicine* 19: 557-566, 2013.
2. **Altshuler D, Hirschhorn JN, Klannemark M, Lindgren CM, Vohl MC, Nemesh J, Lane CR, Schaffner SF, Bolk S, Brewer C, Tuomi T, Gaudet D, Hudson TJ, Daly M, Groop L, and Lander ES**. The common PPARgamma Pro12Ala polymorphism is associated with decreased risk of type 2 diabetes. *Nature genetics* 26: 76-80, 2000.
3. **Amin RH, Mathews ST, Camp HS, Ding L, and Leff T**. Selective activation of PPARgamma in skeletal muscle induces endogenous production of adiponectin and protects mice from diet-induced insulin resistance. *American journal of physiology Endocrinology and metabolism* 298: E28-37, 2010.
4. **Anders S, Pyl PT, and Huber W**. HTSeq--a Python framework to work with high-throughput sequencing data. *Bioinformatics* 31: 166-169, 2015.
5. **Barish GD, Narkar VA, and Evans RM**. PPAR delta: a dagger in the heart of the metabolic syndrome. *The Journal of clinical investigation* 116: 590-597, 2006.
6. **Barroso I, Gurnell M, Crowley VE, Agostini M, Schwabe JW, Soos MA, Maslen GL, Williams TD, Lewis H, Schafer AJ, Chatterjee VK, and O'Rahilly S**. Dominant negative mutations in human PPARgamma associated with severe insulin resistance, diabetes mellitus and hypertension. *Nature* 402: 880-883, 1999.
7. **Bluher M**. Adipose tissue dysfunction in obesity. *Experimental and clinical endocrinology & diabetes : official journal, German Society of Endocrinology [and] German Diabetes Association* 117: 241-250, 2009.

8. **Bosma M, Hesselink MK, Sparks LM, Timmers S, Ferraz MJ, Mattijssen F, van Beurden D, Schaart G, de Baets MH, Verheyen FK, Kersten S, and Schrauwen P**. Perilipin 2 improves insulin sensitivity in skeletal muscle despite elevated intramuscular lipid levels. *Diabetes* 61: 2679-2690, 2012.
9. **Braissant O, Foufelle F, Scotto C, Dauca M, and Wahli W**. Differential expression of peroxisome proliferator-activated receptors (PPARs): tissue distribution of PPAR-alpha, -beta, and -gamma in the adult rat. *Endocrinology* 137: 354-366, 1996.
10. **Buchner DA, Charrier A, Srinivasan E, Wang L, Paulsen MT, Ljungman M, Bridges D, and Saltiel AR**. Zinc Finger Protein 407 (ZFP407) Regulates Insulin-stimulated Glucose Uptake and Glucose Transporter 4 (Glut4) mRNA. *The Journal of biological chemistry* 290: 6376-6386, 2015.
11. **Claussnitzer M, Dankel SN, Klocke B, Grallert H, Glunk V, Berulava T, Lee H, Oskolkov N, Fadista J, Ehlers K, Wahl S, Hoffmann C, Qian K, Ronn T, Riess H, Muller-Nurasyid M, Bretschneider N, Schroeder T, Skurk T, Horsthemke B, Diagram+Consortium, Spieler D, Klingenspor M, Seifert M, Kern MJ, Mejhert N, Dahlman I, Hansson O, Hauck SM, Bluher M, Arner P, Groop L, Illig T, Suhre K, Hsu YH, Mellgren G, Hauner H, and Laumen H**. Leveraging cross-species transcription factor binding site patterns: from diabetes risk loci to disease mechanisms. *Cell* 156: 343-358, 2014.
12. **DeFronzo RA, Ferrannini E, Sato Y, Felig P, and Wahren J**. Synergistic interaction between exercise and insulin on peripheral glucose uptake. *The Journal of clinical investigation* 68: 1468-1474, 1981.
13. **Dunn SE, and Michel RN**. Coordinated expression of myosin heavy chain isoforms and metabolic enzymes within overloaded rat muscle fibers. *The American journal of physiology* 273: C371-383, 1997.
14. **Fang B, Mane-Padros D, Bolotin E, Jiang T, and Sladek FM**. Identification of a binding motif specific to HNF4 by comparative analysis of multiple nuclear receptors. *Nucleic acids research* 40: 5343-5356, 2012.
15. **Finck BN, Bernal-Mizrachi C, Han DH, Coleman T, Sambandam N, LaRiviere LL, Holloszy JO, Semenkovich CF, and Kelly DP**. A potential link between muscle peroxisome proliferator- activated receptor-alpha signaling and obesity-related diabetes. *Cell metabolism* 1: 133-144, 2005.
16. **Furth PA, Hennighausen L, Baker C, Beatty B, and Woychick R**. The variability in activity of the universally expressed human cytomegalovirus immediate early gene 1 enhancer/promoter in transgenic mice. *Nucleic acids research* 19: 6205-6208, 1991.
17. **Gene Ontology C**. Gene Ontology Consortium: going forward. *Nucleic acids research* 43: D1049-1056, 2015.
18. **Hevener AL, He W, Barak Y, Le J, Bandyopadhyay G, Olson P, Wilkes J, Evans RM, and Olefsky J**. Muscle-specific Pparg deletion causes insulin resistance. *Nature medicine* 9: 1491-1497, 2003.
19. **Hill-Baskin AE, Markiewski MM, Buchner DA, Shao H, DeSantis D, Hsiao G, Subramaniam S, Berger NA, Croniger C, Lambris JD, and Nadeau JH**. Diet-induced hepatocellular carcinoma in genetically predisposed mice. *Human molecular genetics* 18: 2975-2988, 2009.

20. **Kersten S, Desvergne B, and Wahli W**. Roles of PPARs in health and disease. *Nature* 405: 421-424, 2000.
21. **Kersten S, Seydoux J, Peters JM, Gonzalez FJ, Desvergne B, and Wahli W**. Peroxisome proliferator-activated receptor alpha mediates the adaptive response to fasting. *The Journal of clinical investigation* 103: 1489-1498, 1999.
22. **Kim D, Pertea G, Trapnell C, Pimentel H, Kelley R, and Salzberg SL**. TopHat2: accurate alignment of transcriptomes in the presence of insertions, deletions and gene fusions. *Genome biology* 14: R36, 2013.
23. **Kim JB, Wright HM, Wright M, and Spiegelman BM**. ADD1/SREBP1 activates PPARgamma through the production of endogenous ligand. *Proceedings of the National Academy of Sciences of the United States of America* 95: 4333-4337, 1998.
24. **Langmead B, and Salzberg SL**. Fast gapped-read alignment with Bowtie 2. *Nature methods* 9: 357-359, 2012.
25. **Li H, Handsaker B, Wysoker A, Fennell T, Ruan J, Homer N, Marth G, Abecasis G, Durbin R, and Genome Project Data Processing S**. The Sequence Alignment/Map format and SAMtools. *Bioinformatics* 25: 2078-2079, 2009.
26. **Love MI, Huber W, and Anders S**. Moderated estimation of fold change and dispersion for RNA-seq data with DESeq2. *Genome biology* 15: 550, 2014.
27. **Norris AW, Chen L, Fisher SJ, Szanto I, Ristow M, Jozsi AC, Hirshman MF, Rosen ED, Goodyear LJ, Gonzalez FJ, Spiegelman BM, and Kahn CR**. Muscle-specific PPARgamma-deficient mice develop increased adiposity and insulin resistance but respond to thiazolidinediones. *The Journal of clinical investigation* 112: 608-618, 2003.
28. **Odom DT, Zizlsperger N, Gordon DB, Bell GW, Rinaldi NJ, Murray HL, Volkert TL, Schreiber J, Rolfe PA, Gifford DK, Fraenkel E, Bell GI, and Young RA**. Control of pancreas and liver gene expression by HNF transcription factors. *Science* 303: 1378-1381, 2004.
29. **Saltiel AR**. Insulin resistance in the defense against obesity. *Cell metabolism* 15: 798-804, 2012.
30. **Shaw JE, Sicree RA, and Zimmet PZ**. Global estimates of the prevalence of diabetes for 2010 and 2030. *Diabetes research and clinical practice* 87: 4-14, 2010.
31. **Si-Tayeb K, Lemaigre FP, and Duncan SA**. Organogenesis and development of the liver. *Developmental cell* 18: 175-189, 2010.
32. **Staiger H, Haas C, Machann J, Werner R, Weisser M, Schick F, Machicao F, Stefan N, Fritsche A, and Haring HU**. Muscle-derived angiopoietin-like protein 4 is induced by fatty acids via peroxisome proliferator-activated receptor (PPAR)-delta and is of metabolic relevance in humans. *Diabetes* 58: 579-589, 2009.
33. **Stephenson EJ, Ragauskas A, Jaligama S, Redd JR, Parvathareddy J, Peloquin MJ, Saravia J, Han JC, Cormier SA, and Bridges D**. Exposure to environmentally persistent free radicals during gestation lowers energy expenditure and impairs skeletal muscle mitochondrial function in adult mice. *American journal of physiology Endocrinology and metabolism* ajpendo 00521 02015, 2016.
34. **Subramanian A, Tamayo P, Mootha VK, Mukherjee S, Ebert BL, Gillette MA, Paulovich A, Pomeroy SL, Golub TR, Lander ES, and Mesirov JP**. Gene set enrichment analysis: a knowledge-based approach for interpreting genome-wide

expression profiles. *Proceedings of the National Academy of Sciences of the United States of America* 102: 15545-15550, 2005.
35. **Sugden MC, Bulmer K, Gibbons GF, Knight BL, and Holness MJ**. Peroxisome-proliferator-activated receptor-alpha (PPARalpha) deficiency leads to dysregulation of hepatic lipid and carbohydrate metabolism by fatty acids and insulin. *The Biochemical journal* 364: 361-368, 2002.
36. **Tan NS, Shaw NS, Vinckenbosch N, Liu P, Yasmin R, Desvergne B, Wahli W, and Noy N**. Selective cooperation between fatty acid binding proteins and peroxisome proliferator-activated receptors in regulating transcription. *Molecular and cellular biology* 22: 5114-5127, 2002.
37. **Tontonoz P, Hu E, Graves RA, Budavari AI, and Spiegelman BM**. mPPAR gamma 2: tissue-specific regulator of an adipocyte enhancer. *Genes & development* 8: 1224-1234, 1994.
38. **Vanttinen M, Nuutila P, Kuulasmaa T, Pihlajamaki J, Hallsten K, Virtanen KA, Lautamaki R, Peltoniemi P, Takala T, Viljanen AP, Knuuti J, and Laakso M**. Single nucleotide polymorphisms in the peroxisome proliferator-activated receptor delta gene are associated with skeletal muscle glucose uptake. *Diabetes* 54: 3587-3591, 2005.
39. **Wang YX, Zhang CL, Yu RT, Cho HK, Nelson MC, Bayuga-Ocampo CR, Ham J, Kang H, and Evans RM**. Regulation of muscle fiber type and running endurance by PPARdelta. *PLoS biology* 2: e294, 2004.
40. **Wu P, Inskeep K, Bowker-Kinley MM, Popov KM, and Harris RA**. Mechanism responsible for inactivation of skeletal muscle pyruvate dehydrogenase complex in starvation and diabetes. *Diabetes* 48: 1593-1599, 1999.

Figure 1. Zfp407 mRNA overexpression in ZFP-TG mice. (A) Endogenous, (B) transgenic and (C) total *Zfp407* mRNA expression was measured by qPCR and normalized to levels of *Arbp* in WT and ZFP-TG (TG) mice (n=4-10 mice per group). * indicates $p < 0.05$, ** indicates a $p < 0.01$ and *** indicates a $p < 0.001$. SQ: Subcutaneous.

Figure 2. Zfp407 protein is overexpressed in heart and muscle of ZFP-TG mice. (A) Transgene construct with mouse Zfp407 cDNA tagged with Myc and DDK. CMV, cytomegalovirus promoter, polyA, human growth hormone polyA signal. (B) ZFP407 and GAPDH protein expression were measured by Western blot in WT and ZFP-TG

561 (TG) mice (n=4-14 mice per group). ** indicates a $p < 0.01$ and *** indicates a $p <$
562 0.001.
563
564 **Figure 3. No morphological differences in muscle and heart tissue between ZFP-TG**
565 **and WT mice.**(A) Muscle and (B) heart tissue from ZFP-TG (TG) and WT mice stained
566 with haemotoxylin and eosin (n=4 mice per group). Total magnification 200x. (C) Gene
567 expression of *Atp2a1* (fast twitch muscle finer marker) and *Atp2a2* (slow twitch muscle
568 fiber marker) in muscle from ZFP-TG and WT male mice (n=5 per group). (D)
569 Representative SDH and (E) GPDHα staining from muscle of ZFP-TG and WT male
570 mice (n=3 per group).
571
572 **Figure 4. ZFP407 overexpression alters the muscle transcriptome.** Gene expression
573 analysis in muscle from ZFP-TG and WT mice (n=5 per group) analyzed by (A)
574 hierarchical clustering of the transcriptome in ZFP-TG and WT mice and (B) volcano
575 plot of gene expression with differentially expressed genes indicated in red. (C) Fold
576 enrichment of gene ontology terms among differentially expressed genes between ZFP-
577 TG and WT mice. (D) Heatmap of gene expression for the PPAR KEGG pathway
578 (03320). ZFP-TG 1-5 and WT 1-5 indicate individual biological replicates. Red indicates
579 decreased relative expression and green indicates increased relative expression.
580
581 **Figure 5. Zfp407 is a pan-PPAR activator.** (A) PPARα, PPARδ, and PPARγ protein
582 levels in muscle of ZFP-TG (TG) and WT mice (n=4 mice per group). (B) A PPAR
583 consensus reporter plasmid was transfected into 293T cells with the following vectors as

584 indicated: pRK5-myc (empty vector control), or cDNA expression vectors encoding
585 Zfp407, PPARα, PPARδ, or PPARγ. (C) Pdk4, Plin2 and Angptl4 mRNA levels as
586 examined by RNA-Seq (n=5 mice per group). * indicates $p < 0.05$ and *** indicates a $p <$
587 0.001.
588
589 **Figure 6. Zfp407 overexpression increases Glut4 expression.** (A) Glut4 mRNA levels
590 as examined by RNA-Seq (n=5 mice per group), (B) Glut4 mRNA levels as examined by
591 qPCR (n=6-12 mice per group), and (C) Glut4 protein levels (n=6-12 mice per group)
592 levels in muscle, heart and subcutaneous adipose tissue of ZFP-TG (TG) and WT mice. *
593 indicates $p < 0.05$ and ** indicates $p < 0.01$.
594
595 **Figure 7. Zfp407 overexpression improves glucose homeostasis of HFD-fed mice.**
596 WT or ZFP-TG (TG) mice were fed CD or HFD beginning at 5 weeks of age. After 86
597 days of CD or HFD feeding, (A) glucose tolerance tests were performed and area under
598 the curve was calculated and (B) insulin tolerance tests were performed. Solid line: CD,
599 dotted line: HFD, open square: WT and closed circle: ZFP-TG. n=7-20 per group.
600
601
602
603

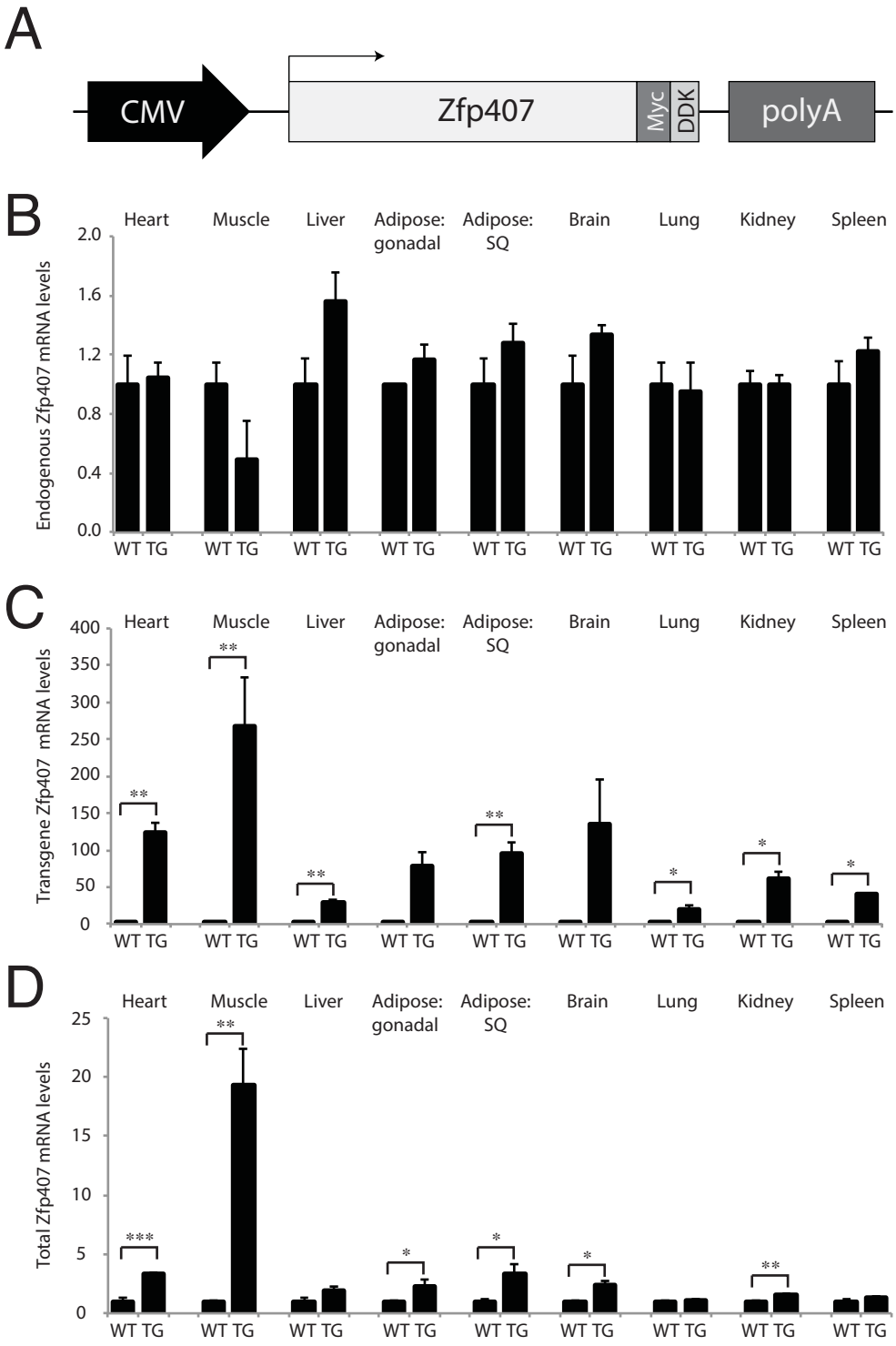
A
CMV
Zfp407
Myc
DDK
polyA
B
Heart
Muscle
Liver
Adipose: gonadal
Adipose: SQ
Brain
Lung
Kidney
Spleen
Endogenous Zfp407 mRNA levels
2.0
1.6
1.2
0.8
0.4
0.0
WT TG
C
Transgene Zfp407 mRNA levels
400
350
300
250
200
150
100
50
0
**
*
D
Total Zfp407 mRNA levels
25
20
15
10
5
0
***

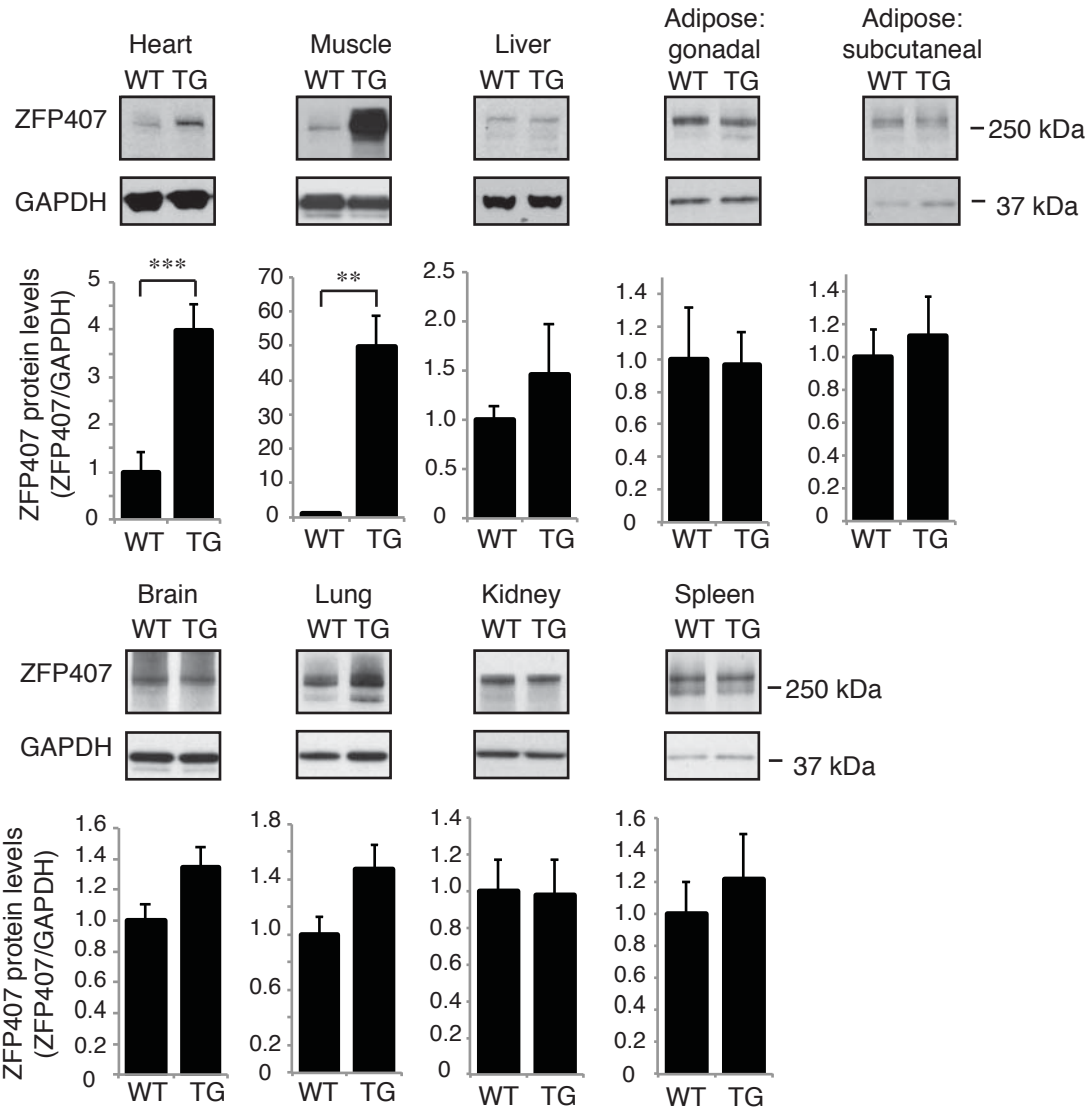
Heart
Muscle
Liver
Adipose: gonadal
Adipose: subcutaneal
WT TG
ZFP407
GAPDH
250 kDa
37 kDa
ZFP407 protein levels (ZFP407/GAPDH)
***
**
Brain
Lung
Kidney
Spleen

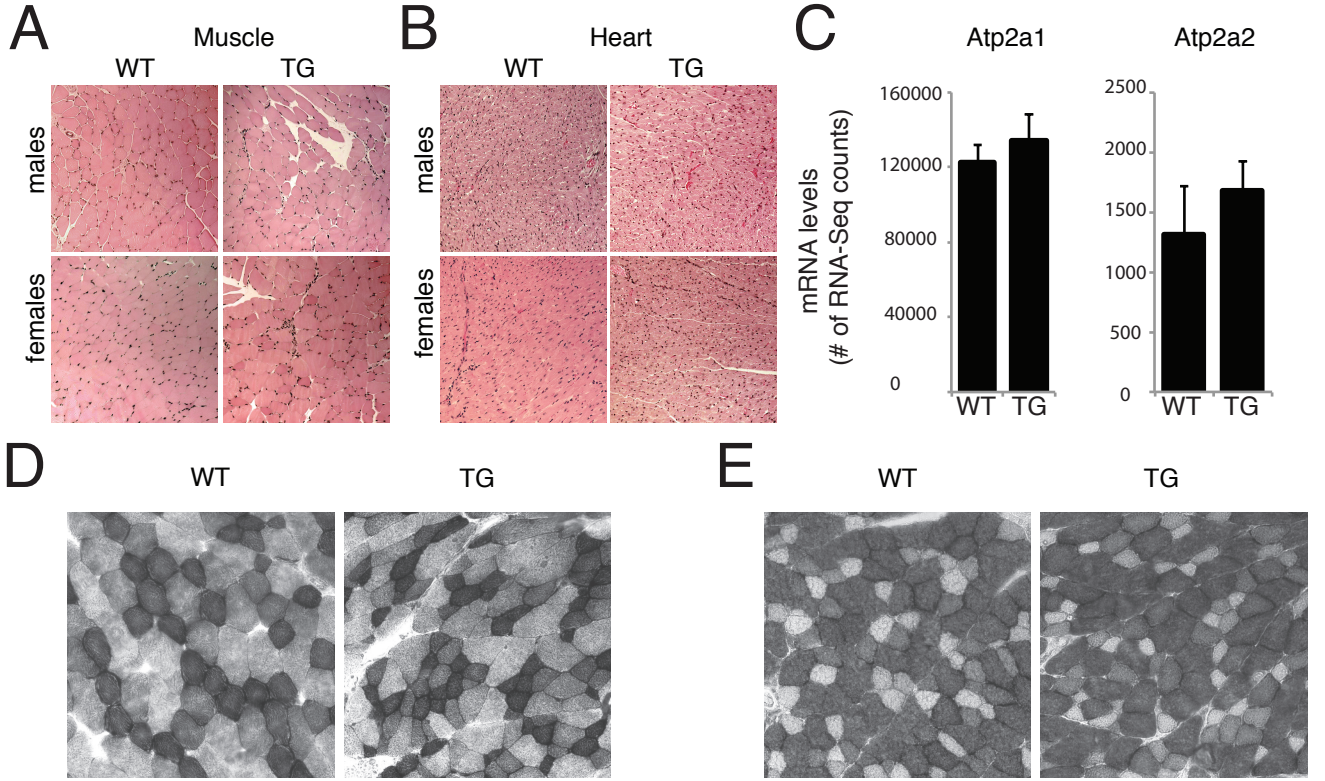
A
Muscle
WT
TG
males
females
B
Heart
WT
TG
males
females
C
Atp2a1
Atp2a2
mRNA levels
(# of RNA-Seq counts)
160000
120000
80000
40000
0
2500
2000
1500
1000
500
0
WT
TG
WT
TG
D
WT
TG
E
WT
TG

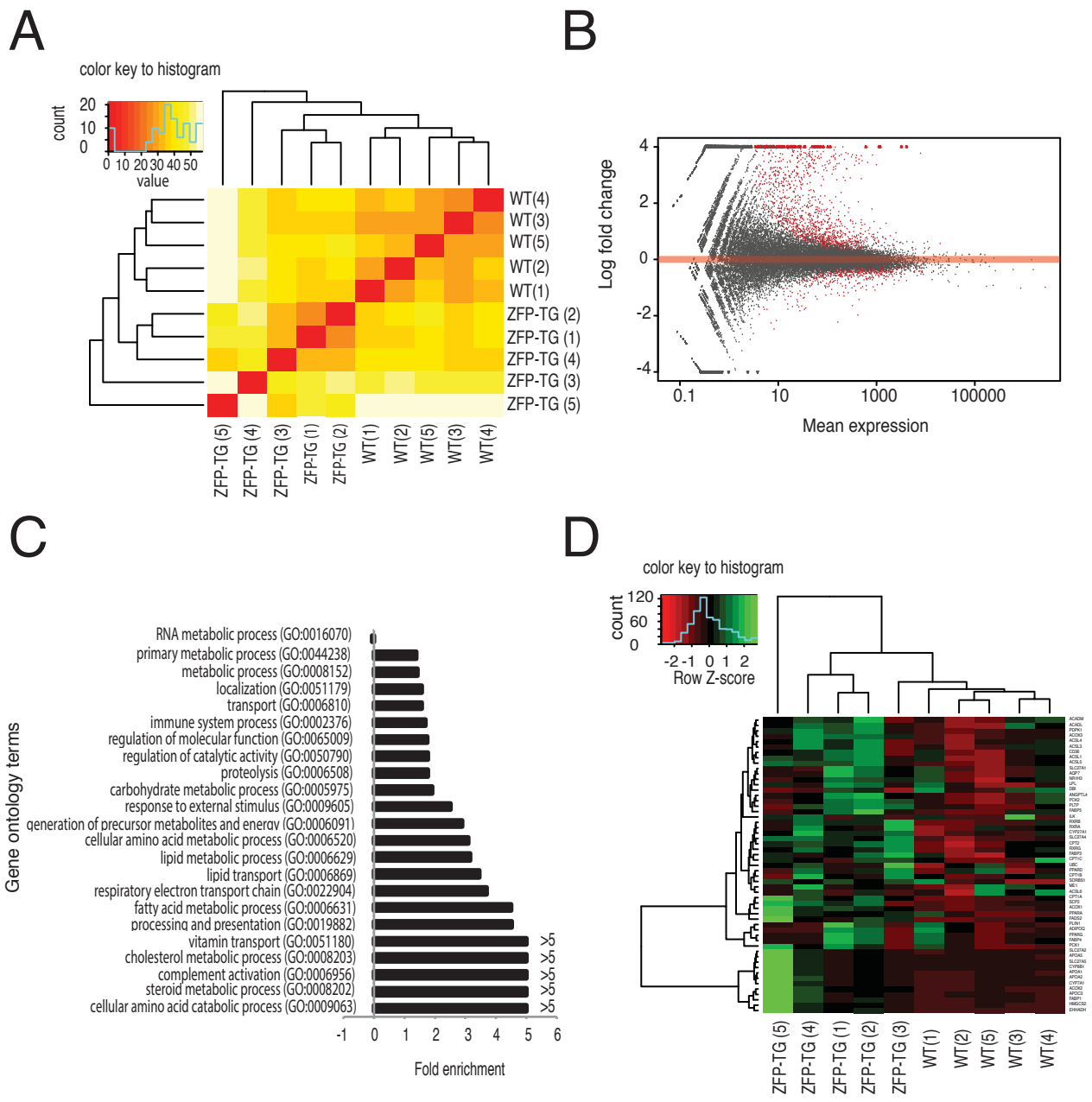
A
color key to histogram
count
20
10
0
0 10 20 30 40 50
value
WT(4)
WT(3)
WT(5)
WT(2)
WT(1)
ZFP-TG (2)
ZFP-TG (1)
ZFP-TG (4)
ZFP-TG (3)
ZFP-TG (5)
ZFP-TG (5)
ZFP-TG (4)
ZFP-TG (3)
ZFP-TG (1)
ZFP-TG (2)
WT(1)
WT(2)
WT(5)
WT(3)
WT(4)
B
Log fold change
4
2
0
-2
-4
0.1
10
1000
100000
Mean expression
C
Gene ontology terms
RNA metabolic process (GO:0016070)
primary metabolic process (GO:0044238)
metabolic process (GO:0008152)
localization (GO:0051179)
transport (GO:0006810)
immune system process (GO:0002376)
regulation of molecular function (GO:0065009)
regulation of catalytic activity (GO:0050790)
proteolysis (GO:0006508)
carbohydrate metabolic process (GO:0005975)
response to external stimulus (GO:0009605)
generation of precursor metabolites and energy (GO:0006091)
cellular amino acid metabolic process (GO:0006520)
lipid metabolic process (GO:0006629)
lipid transport (GO:0006869)
respiratory electron transport chain (GO:0022904)
fatty acid metabolic process (GO:0006631)
processing and presentation (GO:0019882)
vitamin transport (GO:0051180)
cholesterol metabolic process (GO:0008203)
complement activation (GO:0006956)
steroid metabolic process (GO:0008202)
cellular amino acid catabolic process (GO:0009063)
>5
>5
>5
>5
>5
-1
0
1
2
3
4
5
6
Fold enrichment
D
color key to histogram
count
120
60
0
-2 -1 0 1 2
Row Z-score
ZFP-TG (5)
ZFP-TG (4)
ZFP-TG (1)
ZFP-TG (2)
ZFP-TG (3)
WT(1)
WT(2)
WT(5)
WT(3)
WT(4)

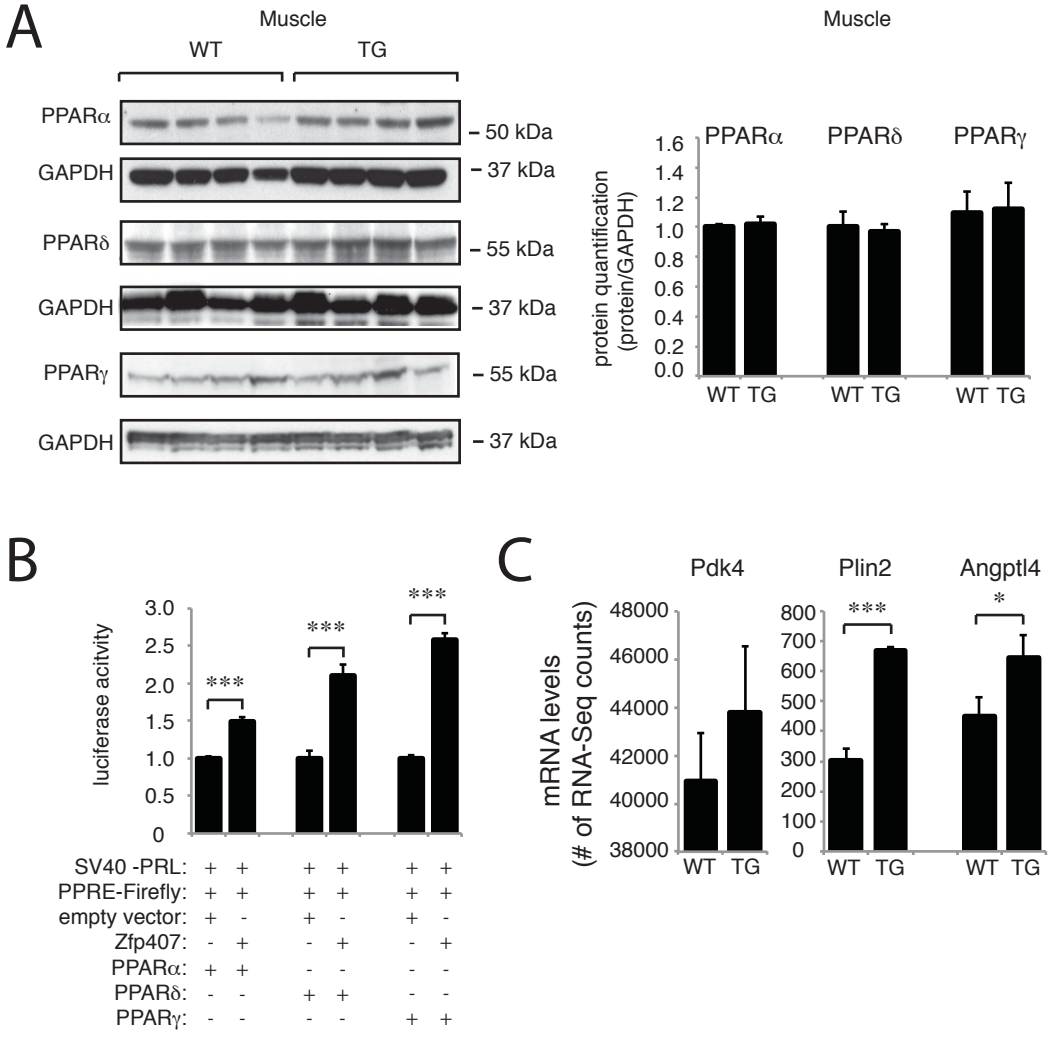
A
Muscle
WT
TG
PPARα
GAPDH
PPARδ
GAPDH
PPARγ
GAPDH
50 kDa
37 kDa
55 kDa
37 kDa
55 kDa
37 kDa
Muscle
PPARα
PPARδ
PPARγ
protein quantification (protein/GAPDH)
1.6
1.4
1.2
1.0
0.8
0.6
0.4
0.2
0.0
WT TG
WT TG
WT TG
B
luciferase acitvity
3.0
2.5
2.0
1.5
1.0
0.5
0
***
***
***
SV40 -PRL: + + + + + +
PPRE-Firefly: + + + + + +
empty vector: + - + - + -
Zfp407: - + - + - +
PPARα: + + - - - -
PPARδ: - - + + - -
PPARγ: - - - - + +
C
Pdk4
Plin2
Angptl4
mRNA levels (# of RNA-Seq counts)
48000
46000
44000
42000
40000
38000
800
700
600
500
400
300
200
100
0
***
*
WT TG
WT TG
WT TG

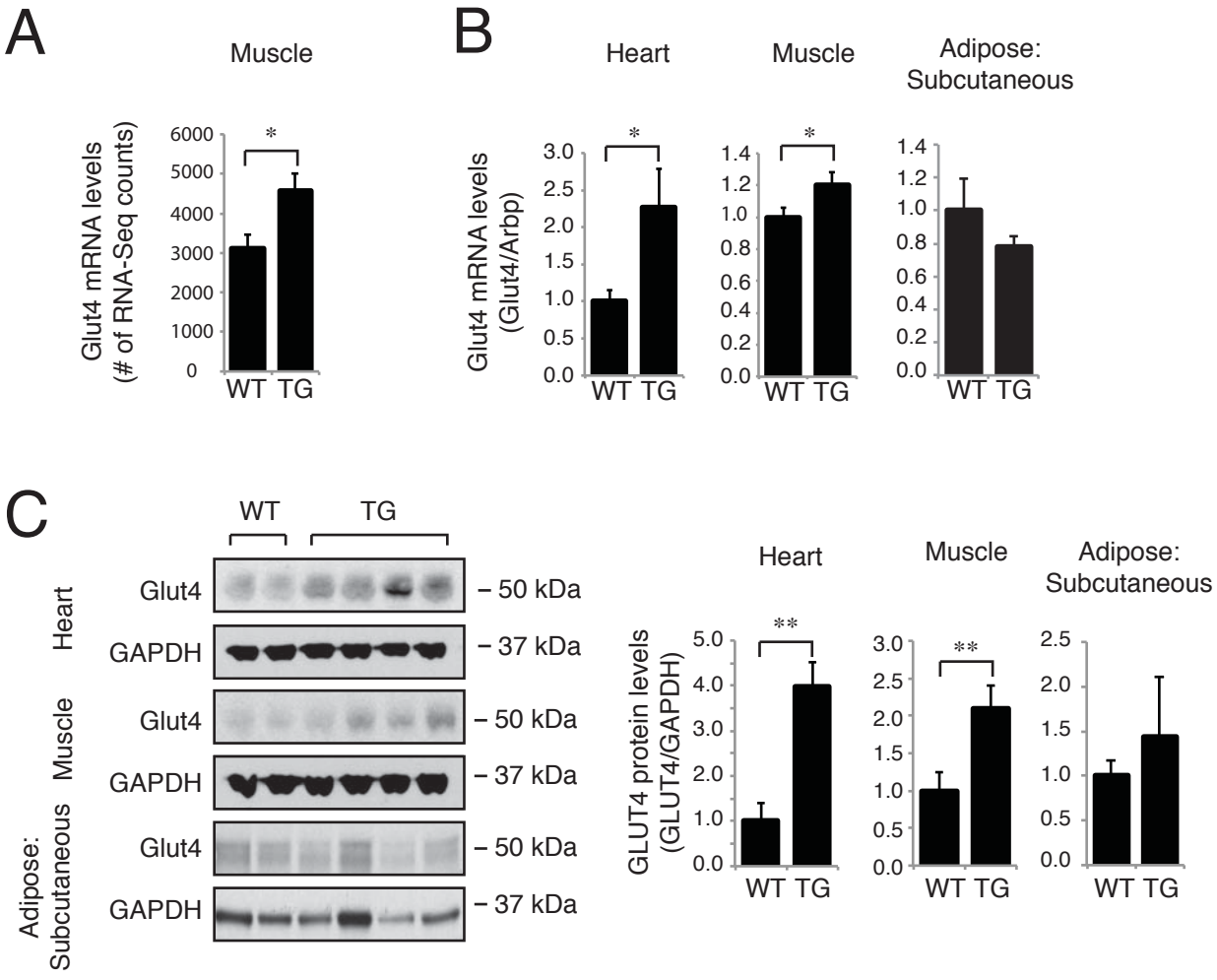
A
Muscle
Glut4 mRNA levels
(# of RNA-Seq counts)
6000
5000
4000
3000
2000
1000
0
*
WT TG
B
Heart
Muscle
Adipose:
Subcutaneous
Glut4 mRNA levels
(Glut4/Arbp)
3.0
2.5
2.0
1.5
1.0
0.5
0.0
1.4
1.2
1.0
0.8
0.6
0.4
0.2
0.0
WT TG
C
WT
TG
Heart
Muscle
Adipose:
Subcutaneous
Glut4
GAPDH
– 50 kDa
– 37 kDa
GLUT4 protein levels
(GLUT4/GAPDH)
5.0
4.0
3.0
2.0
1.0
0.0
2.5
1.5
**

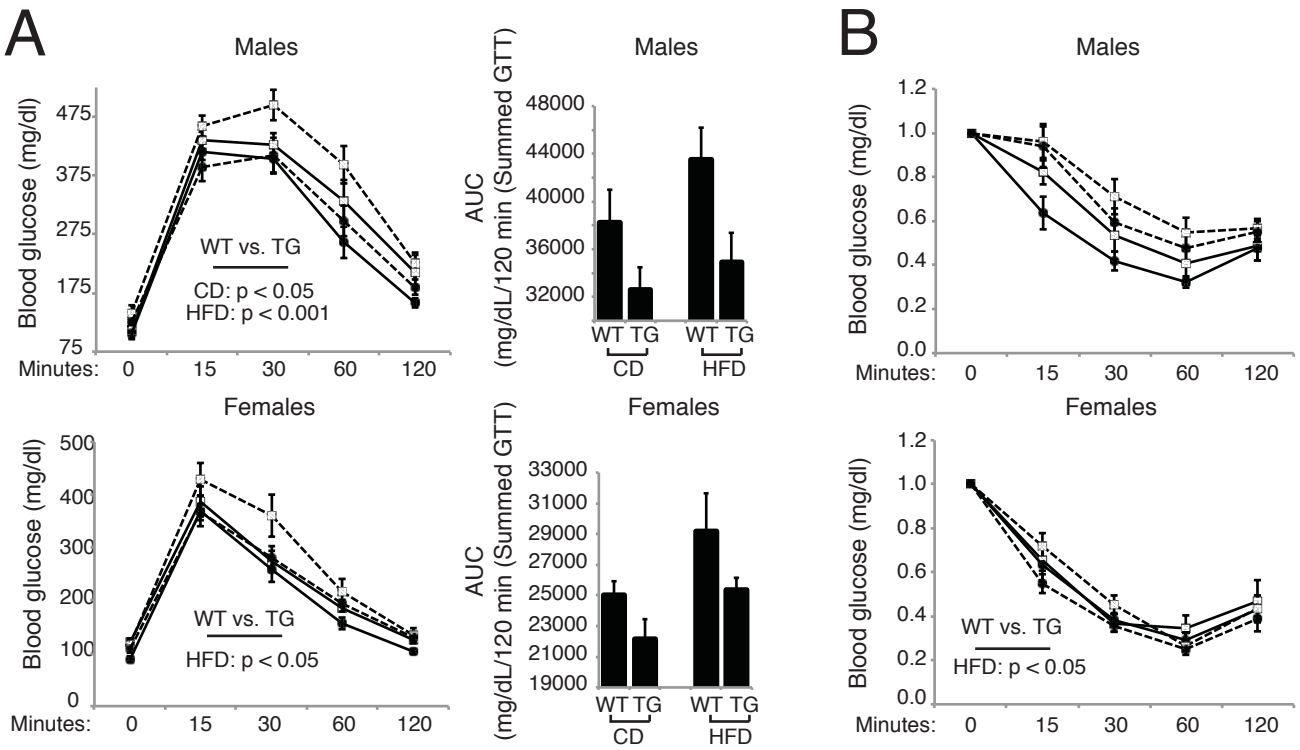
A
Males
Blood glucose (mg/dl)
475
375
275
175
75
Minutes: 0 15 30 60 120
WT vs. TG
CD: p < 0.05
HFD: p < 0.001
Males
AUC
(mg/dL/120 min (Summed GTT)
48000
44000
40000
36000
32000
WT TG WT TG
CD HFD
Females
Blood glucose (mg/dl)
500
400
300
200
100
0
Minutes: 0 15 30 60 120
WT vs. TG
HFD: p < 0.05
Females
AUC
(mg/dL/120 min (Summed GTT)
33000
31000
29000
27000
25000
23000
21000
19000
WT TG WT TG
CD HFD
B
Males
Blood glucose (mg/dl)
1.2
1.0
0.8
0.6
0.4
0.2
0.0
Minutes: 0 15 30 60 120
Females
Blood glucose (mg/dl)
1.2
1.0
0.8
0.6
0.4
0.2
0.0
WT vs. TG
HFD: p < 0.05
Minutes: 0 15 30 60 120

Table 1. Metabolic trait data in 5-week old ZFP-TG and WT mice.

Sex	Trait	WT	SEM	n	ZFP-TG	SEM	n	2-Way ANOVA		
								Genotype	Sex	Interactions
Males	Body Weight (g)	20.39	0.22	66	18.29	0.33	60	2.30E-09	< 2.2e-16	N.S.
	Length (mm)	86.54	0.68	35	86.04	0.86	23	0.04645	7.68E-05	N.S.
	Body mass index (kg/m2)	2.71	0.38	29	2.60	0.22	27	N.S.	1.30E-11	N.S.
	Fasting glucose (mg/dl)	103.57	3.59	30	83.22	4.60	23	1.02E-05	4.22E-05	N.S.
	Fasting insulin (ng/ml)	0.41	0.07	19	0.14	0.02	9	0.000623	N.S.	N.S.
	HOMA-IR	3.07	0.68	19	0.83	0.15	9	1.87E-05	N.S.	N.S.
	Plasma beta-hydroxybutyrate (mg/dl)	14.35	1.36	11	19.90	1.28	9	0.0002121	N.S.	N.S.
	Plasma cholesterol (mg/dl)	100.73	3.21	11	98.00	3.98	9	N.S.	1.28E-07	N.S.
	Plasma nonesterified fatty acids (mg/dl)	0.92	0.08	11	0.97	0.07	9	N.S.	0.02075	N.S.
	Plasma triglycerides (mg/dl)	140.18	15.85	11	149.89	12.78	9	N.S.	8.01E-05	N.S.
	Muscle triglycerides (mg/g tissue)	9.44	1.64	5	9.46	1.51	5	N.S.	N.S.	N.S.
Females	Body Weight (g)	16.70	0.18	48	15.56	0.25	41	2.30E-09	< 2.2e-16	N.S.
	Length (mm)	84.48	0.48	27	82.05	0.60	19	0.04645	7.68E-05	N.S.
	Body mass index (kg/m2)	2.36	0.39	25	2.30	1.04	17	N.S.	1.30E-11	N.S.
	Fasting glucose (mg/dl)	86.00	4.10	28	64.06	4.81	17	1.02E-05	4.22E-05	N.S.
	Fasting insulin (ng/ml)	0.39	0.06	16	0.23	0.07	11	0.000623	N.S.	N.S.
	HOMA-IR	2.46	0.38	16	0.98	0.27	11	1.87E-05	N.S.	N.S.
	Plasma beta-hydroxybutyrate (mg/dl)	16.46	1.46	10	23.25	1.91	10	0.0002121	N.S.	N.S.
	Plasma cholesterol (mg/dl)	71.90	4.82	10	71.00	4.92	10	N.S.	1.28E-07	N.S.
	Plasma nonesterified fatty acids (mg/dl)	1.46	0.30	10	1.46	0.25	10	N.S.	0.02075	N.S.
	Plasma triglycerides (mg/dl)	85.80	6.80	10	98.80	8.87	10	N.S.	8.01E-05	N.S.
	Muscle triglycerides (mg/g tissue)	10.80	1.29	5	11.70	1.84	5	N.S.	N.S.	N.S.

Table 2. Metabolic trait data for CD- or HFD-fed 135-day old ZFP-TG and WT male mice.

Trait	Diet												3-Way ANOVA			
	CD						HFD						Genotype	Sex	Diet	Interactions
	WT	SEM	n	ZFP-TG	SEM	n	WT	SEM	n	ZFP-TG	SEM	n	p-value			
Body Weight (g)	29.09	0.50	18	25.80	0.53	14	38.63	1.69	20	32.89	1.41	16	3.81E-06	< 2.2e-16	9.08E-13	Sex:Diet p = 0.005
Total weight gained (g)	8.53	0.51	16	7.01	0.64	11	18.36	1.42	20	14.66	1.08	16	1.80E-03	4.11E-14	3.72E-16	Sex:Diet p < 0.001
Percent weight gained (%)	41.87	2.87	16	39.83	5.02	11	89.78	6.13	20	82.47	7.03	16	N.S.	1.10E-08	1.73E-15	Sex:Diet p = 0.006
Percent fat mass (%)	17.91	0.92	14	17.62	1.08	10	26.20	1.56	20	23.27	1.75	16	N.S.	0.001773	3.62E-07	N.S.
Percent lean mass (%)	82.09	0.92	14	82.38	1.08	10	73.80	1.56	20	76.73	1.75	16	N.S.	0.01034	6.13E-08	N.S.
Perigonadal fat mass (g)	0.27	0.04	14	0.24	0.05	10	0.95	0.12	20	0.71	0.13	14	0.034161	3.77E-08	7.08E-08	Sex:Diet p = 0.003
Inguinal fat mass (g)	0.16	0.03	14	0.15	0.02	10	0.60	0.08	20	0.43	0.07	14	0.032657	5.23E-06	8.42E-09	Sex:Diet p = 0.008
Length (mm)	98.94	0.62	19	95.93	0.89	14	102.00	0.57	16	100.86	1.14	14	0.005326	0.002286	5.20E-08	Genotype:Diet p = 0.03
Body mass index (kg/m2)	3.00	0.63	18	2.86	0.84	16	3.71	1.40	20	3.20	0.91	15	5.87E-06	< 2.2e-16	4.46E-09	Genotype:Diet p = 0.03
Fasting glucose (mg/dl)	96.71	4.98	18	84.29	5.45	14	145.85	8.51	20	132.69	8.55	16	2.25E-02	0.01764	1.21E-09	Genotype:Diet p = 0.03
Fasting insulin (ng/ml)	0.34	0.06	8	0.23	0.06	7	0.44	0.11	10	0.35	0.07	9	N.S.	N.S.	N.S.	N.S.
HOMA-IR	2.10	0.41	8	1.54	0.51	7	3.69	0.75	10	3.44	0.88	9	N.S	0.01524	0.03014	N.S.
GTT AUC	38270	2719	8	32610	1851	7	43551	2636	10	34917	2343	9	0.0008729	8.31E-13	0.0078087	N.S.
Plasma beta-hydroxybutyrate (mg/dl)	21.01	0.97	9	17.21	1.69	9	13.56	1.57	10	12.50	1.52	9	N.S.	0.011259	0.002899	N.S.
Plasma cholesterol (mg/dl)	121.56	5.58	9	117.22	10.00	9	145.70	14.37	10	122.33	10.70	9	0.03804	2.24E-05	N.S.	N.S.
Plasma nonesterified fatty acids (mg/dl)	138.00	9.99	9	113.44	10.19	9	117.40	11.84	10	97.33	7.37	9	N.S.	N.S.	N.S.	N.S.
Plasma triglycerides (mg/dl)	1.07	0.03	9	1.11	0.06	9	0.90	0.05	10	1.09	0.12	8	0.008887	2.06E-05	0.024818	N.S.

Table 3. Metabolic trait data for CD- or HFD-fed 135-day old ZFP-TG and WT female mice.

Trait	Diet												3-Way ANOVA			
	CD						HFD						Genotype	Sex	Diet	Interactions
	WT	SEM	n	ZFP-TG	SEM	n	WT	SEM	n	ZFP-TG	SEM	n	p-value			
Body Weight (g)	22.33	0.67	14	19.58	0.50	11	25.47	0.91	10	23.70	0.91	13	3.81E-06	< 2.2e-16	9.08E-13	Sex:Diet p = 0.005
Total weight gained (g)	4.70	0.46	10	4.21	0.42	11	8.86	0.61	13	8.01	0.65	13	1.80E-03	4.11E-14	3.72E-16	Sex:Diet p < 0.001
Percent weight gained (%)	30.42	3.54	9	27.69	3.58	10	53.12	3.80	13	51.93	4.65	13	N.S.	1.10E-08	1.73E-15	Sex:Diet p = 0.006
Percent fat mass (%)	16.67	0.38	10	16.45	0.72	10	21.48	1.46	10	19.38	1.69	11	N.S.	0.001773	3.62E-07	N.S.
Percent lean mass (%)	83.33	0.38	10	83.55	0.72	10	77.53	1.62	10	79.23	1.72	11	N.S.	0.01034	6.13E-08	N.S.
Perigonadal fat mass (g)	0.11	0.01	10	0.10	0.01	10	0.24	0.06	9	0.22	0.06	10	0.034161	3.77E-08	7.08E-08	Sex:Diet p = 0.003
Inguinal fat mass (g)	0.11	0.01	10	0.10	0.01	10	0.23	0.04	9	0.21	0.04	10	0.032657	5.23E-06	8.42E-09	Sex:Diet p = 0.008
Length (mm)	97.74	0.99	19	94.27	0.73	11	99.00	0.60	14	98.88	11.60	16	0.005326	0.002286	5.20E-08	Genotype:Diet p = 0.03
Body mass index (kg/m2)	2.31	0.53	11	2.24	0.77	11	2.69	0.76	14	2.43	0.68	16	5.87E-06	< 2.2e-16	4.46E-09	Genotype:Diet p = 0.03
Fasting glucose (mg/dl)	104.71	7.66	14	74.00	6.43	11	113.62	7.95	13	114.57	0.65	14	2.25E-02	0.01764	1.21E-09	Genotype:Diet p = 0.03
Fasting insulin (ng/ml)	0.26	0.06	9	0.31	0.07	7	0.27	0.05	9	0.22	0.06	8	N.S.	N.S.	N.S.	N.S.
HOMA-IR	1.79	0.42	9	1.65	0.34	7	2.14	0.43	9	1.47	0.40	8	N.S	0.01524	0.03014	N.S.
GTT AUC	24995	937	9	22145	1312	7	29168	2467	9	25336	803	8	0.0008729	8.31E-13	0.0078087	N.S.
Plasma beta-hydroxybutyrate (mg/dl)	20.23	2.23	9	19.65	2.03	11	17.72	1.51	10	18.90	1.62	11	N.S.	0.011259	0.002899	N.S.
Plasma cholesterol (mg/dl)	95.44	5.06	9	96.36	4.93	11	109.60	7.92	10	90.00	8.29	11	0.03804	2.24E-05	N.S.	N.S.
Plasma nonesterified fatty acids (mg/dl)	96.78	6.67	9	91.64	3.62	11	90.70	6.89	10	84.36	7.21	11	N.S.	N.S.	N.S.	N.S.
Plasma triglycerides (mg/dl)	0.98	0.08	9	1.26	0.19	11	1.23	0.33	10	0.95	0.10	10	0.008887	2.06E-05	0.024818	N.S.
Muscle triglycerides (mg/g tissue)	N.D.			N.D.			12.18	2.26	4	15.47	2.10	5	N.S.	N.D.	N.D.	N.D.